HHS Public Access

Author manuscript

Plant J. Author manuscript; available in PMC 2019 October 30.

Published in final edited form as:

Plant J. 2018 October ; 96(2): 316–328. doi:10.1111/tpj.14032.

Characterization of filament-forming CTP synthases from *Arabidopsis thaliana*

Manuel Daumann[1], **Daniel Hickl**[1], **David Zimmer**[1], **Rachael A. DeTar**[2], **Hans-Henning Kunz**[2,*], **Torsten Möhlmann**[1,*]

[1]Pflanzenphysiologie, Fachbereich Biologie, Universität Kaiserslautern, Erwin-Schrodinger-Straße, D-67663, Kaiserslautern, Germany, and [2]School of Biological Sciences, Washington State University, PO Box 644236, Pullman, WA, 99164-4236, USA

SUMMARY

Cytidine triphosphate (CTP) is essential for DNA, RNA and phospholipid biosynthesis. *De novo* synthesis is catalyzed by CTP synthases (CTPS). Arabidopsis encodes five CTPS isoforms that unanimously share conserved motifs found across kingdoms, suggesting all five are functional enzymes. Whereas *CTPS1–4* are expressed throughout Arabidopsis tissues, *CTPS5* reveals exclusive expression in developing embryos. CTPS activity and substrates affinities were determined for a representative plant enzyme on purified recombinant CTPS3 protein. As demonstrated in model organisms such as yeast, fruit fly and mammals, CTPS show the capacity to assemble into large filaments called cytoophidia. Transient expression of N- and C-terminal *YFP-CTPS* fusion proteins in *Nicotiana benthamiana* allowed to monitor such filament formation. Interestingly, CTPS1 and 2 always appeared as soluble proteins, whereas filaments were observed for CTPS3, 4 and 5 independent of the YFP-tag location. However, when similar constructs were expressed in *Saccharomyces cerevisiae*, no filaments were observed, pointing to a requirement for organism-specific factors *in vivo*. Indications for filament assembly were also obtained *in vitro* when recombinant CTPS3 protein was incubated in the presence of CTP. T-DNA-insertion mutants in four *CTPS* loci revealed no apparent phenotypical alteration. In contrast, *CTPS2* T-DNA-insertion mutants did not produce homozygous progenies. An initial characterization of the CTPS protein family members from Arabidopsis is presented. We provide evidence for their involvement in nucleotide *de novo* synthesis and show that only three of the five CTPS isoforms were able to form filamentous structures in the transient tobacco expression system. This represents a striking difference from previous observations in prokaryotes, yeast, Drosophila and

*For correspondence (henning.kunz@wsu.edu; moehlmann@biologie.uni-kl.de).

AUTHOR CONTRIBUTIONS

Conceptualization: H.-H.K and T.M.; methodology: H.H.K., M.D., T.M.; investigation: M.D. (T-DNA insertion mutant screen, filament formation studies *in vitro* and *in planta*), D.H. (knockout mutant screens and expression studies in yeast), D.Z. (protein production, activity assay, mutational analysis), H.-H.K. with help from R.A.D. (cloning of genes and preparation of fluorescent fusion protein constructs). T.M. and H.-H.K wrote the manuscript.

CONFLICT OF INTEREST

The authors declare no conflict of interest.

SUPPORTING INFORMATION

Additional Supporting Information may be found in the online version of this article.

mammalian cells. This finding will be highly valuable to further understand the role of filament formation to regulate CTPS activity.

Keywords

filaments; cytoophidia; cytidine triphosphate synthase; pyrimidine; *de novo* synthesis; yeast

INTRODUCTION

The ATP-dependent synthesis of cytidine triphosphate (CTP) from UTP represents a universal biochemical reaction found in prokaryotes and eukaryotes (Liebermann, 1956; Long and Pardee, 1967; Wadskov-Hansen *et al.*, 2001; Evans and Guy, 2004). The reaction is exclusively catalyzed by an enzyme designated as CTP synthase (CTPS) finalizing the pyrimidine *de novo* synthesis pathway. Newly formed CTP (dCTP) molecules represent building blocks for nucleic acids, and thus are essential for gene transcription and for nucleic acid synthesis during cell division. In addition, CTP can also act as a cofactor in fundamental biochemical pathways, for instance in the eukaryotic phospholipid biosynthesis to produce the intermediate compound CDP-choline or during coenzyme A production, which involves CTP hydrolysis.

To guarantee appropriate CTP supply in a timely manner, a tight regulation of CTPS enzyme activity is key. In addition, such regulation is required to avoid depletion of ATP and UTP pools. Accordingly, CTPS is regulated on several levels: transcriptionally, post-translationally via phosphorylation, allosterically (activated) by guanosine triphosphate (GTP) and feedback inhibited by its own product CTP. Besides these commonly observed mechanisms, a new potential CTPS regulatory mechanism was discovered recently in bacteria, fungi, fruit flies and mammals. Using fluorescence fusion proteins and immunology, independent research from a variety of diverse organisms, revealed that CTPS proteins have the capacity to form filaments both *in vivo* and *in vitro* (Ingerson-Mahar *et al.*, 2010; Noree *et al.*, 2010; Liu, 2010; Lynch *et al.*, 2017). CTPS filaments from *Escherichia coli* represent an inactive conformation of the CTPS enzyme complex, which was determined by assaying CTPS polymerization and simultaneously quantifying its enzymatic activity in *E. coli* (Barry *et al.*, 2014). This result is supported by others who observed a downregulation of activity by cytoophidia formation (Aughey *et al.*, 2014; Noree *et al.*, 2014). In contrast, crystallization of the human CTPS filaments revealed ploymerization in the active conformation (Lynch *et al.*, 2017).

The amino acid sequences of CTPSs are highly conserved among divergent organisms and consist of two domains: (i) the N-terminal ALase domain, where the substrate UTP is transiently phosphorylated by ATP; and (ii) the GATase domain where this phosphate group is exchanged with ammonia from Gln (Endrizzi *et al.*, 2004). In order to switch into the active state, CTPS first dimerizes and eventually organizes into homotetramers, the active enzyme form (Levitzki and Koshland, 1972; Barry *et al.*, 2014). The tetramerization step is strongly dependent on substrate availability, i.e. both ATP and UTP. Once the product CTP

is formed, the reaction becomes feedback inhibited (Ingerson-Mahar *et al.*, 2010; Noree *et al.*, 2010; Liu, 2011).

These phenomena have been studied in various bacteria and eukaryotes; however, there is a debate about their function for cell physiology. Moreover, no data exist regarding the molecular identity or the structural characteristics of CTPS from plants or algae thus far. This is interesting because photoautotrophic eukaryotic cells are in some respect more complex than fungi and animal cells. Besides the mitochondrium they contain a second type of organelle with endosymbiotic origin, the plastid that is home to the photosynthetic machinery. Because plastids possess their own genome, the plastome, which expresses vital genes and needs to be replicated whenever plastids divide, a coordinated supply of CTP to the organelle is vital for the entire organism.

By performing a sequence-based homology search we identified five loci in the genome of the model plant *Arabidopsis thaliana* that encode for putative CTPS homologs. Here, we present data on the successful cloning, localization and initial characterization of the CTPSs from *A. thaliana*. Using transient expression assays in *Nicotiana benthamiana* we show that under the tested conditions not all of the five CTPS members form cytosolic filaments *in vivo*. Thus far, similar observations have only been reported from Drosophila where two out of three alternative splice versions encoded in one *CTPS* locus produced non-filamentous CTPS proteins in a tissue-specific and developmental-dependent fashion (Azzam and Liu, 2013). In addition, we heterologously expressed and purified the candidate proteins and confirmed CTPS activity by detailed biochemical characterization of one representative, CTPS3. Lastly, with the exception of *CTPS2*, we successfully isolated homozygous single T-DNA insertion mutants that did not reveal phenotypic changes from wild-type controls under standard short- and long-day growth conditions. Interestingly, for *CTPS2* no homozygous T-DNA insertion line could be identified, implying a highly specific developmental role for this isoform.

RESULTS

Arabidopsis possesses five putative CTPS isoforms

The genome of the reference plant *A. thaliana* encodes for five putative CTPS genes, distributed on chromosomes 1, 2, 3 and 4. Deduced proteins contain between 556 and 600 amino acids, and share between 64.8% and 74% sequence identity among each other. There is a significant similarity between these five candidate proteins from plants and CTPSs from *Saccharomyces cerevisiae* (URA7, URA8), *Homo sapiens* (CTPS1, CTPS2) and *Drosophila melanogaster* (isoform A, isoform B) of between 45 and 58.5% (Table 1). In addition, the domains required for GATase and ALase activity, including highly conserved amino acids, were found to be present in all five Arabidopsis proteins, indicating that all five members may possess CTPS activity *in vivo* (Figure 1).

Subsequently, publicly available microarray gene expression data were consulted to gain insights into the predominant *CTPS* genes expressed in a given tissue (AtGenexpress; Schmid *et al.*, 2005; Figure S1). Based on the level of expression, genes were designated as *CTPS1* the strongest expressed gene of all five isoforms to *CTPS5* the lowest expressed

locus. Whereas on average *CTPS1–3* reveal high expression in all analyzed tissues, *CTPS4* is barely expressed in leaves but peaks in the shoot apex and flower organs. Lastly, *CTPS5* is expressed in very low levels exclusively in the seed endosperm but is absent in other tissues tested (Figure S1).

A commercially available CTPS antibody (Santa Cruz sc-134457, www.scbt.com) raised against a conserved CTPS peptide was employed to verify total CTPS protein expression in various Arabidopsis tissues. While detection of corresponding 55–70-kDA bands in seedlings and floral tissues was low, siliques showed more intense signals, implying higher *CTPS* expression in corresponding tissues (Figure 2a). In general, relative long exposure times were required to detect CTPS in tissue whole-protein extracts. However, this was not due to poor antibody-binding affinities to the plant CTPS members as proper signals were observed using purified, recombinant protein controls (Figure 2b). *In situ* hybridization experiments with Arabidopsis roots in whole-mount technique did not allow detection of CTPS protein or any filament structures so far.

Arabidopsis CTPSs 3, 4 and 5 are able to form filamentous protein structures

Cytidine triphosphate synthases from diverse bacteria and eukaryotes share the capability to form filaments or so-called cytoophidia in the cytosol. To check whether Arabidopsis CTPSs share the feature to form filamentous structures and to verify their subcellular protein localizations, the corresponding cDNAs for *CTPS1–4* were amplified and cloned. In the case of *CTPS5* a genomic DNA construct was built as *CTPS5* gene expression was too low in all tissue-specific RNA extractions to successfully amplify a *CTPS5* cDNA fragment. All cDNA or genomic DNA *CTPS* reading frame fragments were either N- or C-terminally fused to YFP to minimize the chance of artificial filament formations. Subsequently, all resulting constructs were transiently expressed in *N. benthamiana* leaves and analyzed by confocal microscopy.

Figure 3 displays representative images for each individually tested CTPS-YFP fusion. All five CTPS gene products accumulated in the cytosol. However, their structural appearance varied significantly. Both CTPS1 and CTPS2 appeared soluble and were uniformly distributed in the cytosol resembling the situation found for an unfused, free YFP control. The solubility of all four CTPS1 and CTPS2 fusion protein variants was found to be independent of upstream or downstream YFP protein fusion. In all cases, no visual filament formation was observed (Figure 3a,b).

This was in clear contrast with the protein structures of CTPS3, CTPS4 and CTPS5 YFP fusions. For all three C-terminal YFP fusion proteins clear filamentous structures were recognizable in the cytosol (Figure 3a). Whereas CTPS3 and 5 showed a blurry appearance of filamentous structures, CTPS4 appeared more dense and with bundles of filaments reaching out in various directions. Swopping YFP from C- to N-terminus influenced the appearance of the filaments. In the case of CTPS3 the cloudy appearance changed into a clear and distinct filament structure as previously observed for other CTPS filaments from various organisms (Liu, 2010; Noree *et al.*, 2010). Cells giving rise to CTPS3 N-term-YFP were packed with high numbers of filaments (Figure 3b). However, only about 1–3% of the transformed and investigated cells revealed such drastic filament accumulation. The majority

of cells showed fewer filaments or a soluble appearance. CTPS4 N-term-YFP exhibits cloudy shaped structures compared with the remarkably dense packed filaments when YFP was present at the C-terminus. In the case of CTPS5 N-term-YFP most of the labeled protein was soluble and only some protein appeared condensed in small foci (Figure 3b). For all constructs, we verified by Western blotting using a YFP-specific antiserum that full-length YFP fusion proteins were synthesized in *N. benthamiana* (Figure S2).

In summary, it seems that the YFP orientation to some degree had an impact on the appearance of the filaments and their frequency. However, for CTPS1 and 2 filament formation was completely absent, whereas for CTPS3, CTPS4 and CTPS5 filamentous structures were observed independent of the YFP localization at the N- or C-terminus. The obtained results indicate that CTPS filament formation is a unique feature restricted to specific Arabidopsis CTPS isoforms. Moreover, the position of reporter genes fused to the CTPS affected filament formation to some degree.

For a further characterization of filament formation we mutated amino acid residues in the linker region of CTPS3, connecting the GATase and ALase domains. This so-called linker-linker interface is reported to be involved in filament formation in pyrG from *E. coli* (Barry *et al.*, 2014). Although there is little conservation with respect to the amino acid sequence, homology modeling suggests the presence of an alpha helix in all Arabidopsis CTPS isoforms as well as in pyrG (Figure S3). A mutational analysis was performed with filament forming CTPS3 C-Term-YFP. After transient expression in *N. benthamiana*, plants synthesizing CTPS3-D280, D282, K286 or E289 individually were monitored for filament formation by confocal laser-scanning microscopy (CLSM) of the lower epidermal leaf tissue. No obvious differences in expression level and filament number per cell were observed in any of the mutants. The appearance of the filament structures was also highly similar between constructs (Figure S3).

No filament formation from *CTPS1–4* after expression in *Saccharomyces cerevisiae*

To verify the functionality of the CTPS-YFP fusion proteins, CTPS3, used before for mutational analysis, was selected to test enzymatic activity of the protein. A CTPS3-YFP fusion construct was expressed in *S. cerevisiae*. Clearly, YFP fluorescence was detected in the corresponding cells. However, no filament formation was observed in these cells. In protein extracts of these cells a fivefold increased CTPS activity was measured compared with control cells without expression construct (Figure S4). The presence of enzymatic activity supports the assumption of CTPS-YFP fusion proteins being properly folded and biochemically functional. Furthermore, neither CTPS1, nor 2 and 4 formed filamentous structures in yeast cells employing the expression system described above. Robust YFP fluorescence together with signals in Western blots clearly confirmed the presence of the fusion proteins (Figures 4 and S4). Interestingly, in our controls in which the endogenous yeast CTPSs *ura7* and *ura8* were expressed, using the same system and grown under the exact same conditions, showed appearance of typical filament structures (Figure 4).

Arabidopsis recombinant CTPS3 exhibits CTPS activity

Although *CTPS3-YFP* could be functionally expressed in *S. cerevisiae*, the activity and purity of the enzyme were not sufficient for a detailed characterization. Therefore, we employed *E. coli* as an alternative expression system for plant *CTPS* isoforms, and subsequently purified the corresponding proteins via a translationally fused N-terminal 10xHis-tag (pET System, Novagen, www.novagen.com). In a screen for expression levels of *CTPS1–4* it turned out that most isoforms performed poorly. However, expression of *CTPS3* was adequate for further purification and functional analysis of the corresponding protein. Because growth at 37°C mainly led to the formation of inclusion bodies, expression was carried out at 16°C overnight after induction to maintain maximum solubility. The resulting protein was purified via IMAC, eluted by a stepwise increasing imidazole gradient and desalted (Figure 5a), resulting in protein yields between 0.5 and 0.9 mg L^{-1}.

To assay CTPS activity for CTPS3 a two-step protocol previously established for *E. coli* was applied (Barry *et al.*, 2014). Firstly, recombinant protein was incubated with buffered UTP for 10 min to allow formation of the functional CTPS protein quaternary structure. Subsequently, all further substrates and effectors were added to the reaction mix. After incubation for a given time the reaction was stopped by heat treatment for 3 min at 95°C, and reaction products were separated and quantified by high-performance liquid chromatography (HPLC). Time-dependent CTP production was almost linear for 45 min (Figure 5b). We carefully tested that no CTP formation was detectable in the absence of glutamine or in the presence of 2.5 mM of the non-metabolizable Gln analog 6-diazo-5-oxo-L-norleucine, respectively. Next, the substrate dependency of CTPS3-catalyzed CTP formation was analyzed. For ATP and Gln Michaelis–Menten kinetics were observed with apparent affinities of 0.32 ± 0.015 and 0.12 ± 0.02 mM, respectively (Figure 6a,b). UTP a sigmoidal curve shape was detected, pointing to a cooperative substrate dependency with an affinity of 0.44 ± 0.1 mM (Figure 6c).

GTP was reported earlier as an activator of CTPS enzymes from *E. coli* (Lunn *et al.*, 2008; Barry *et al.*, 2014). Indeed, also the CTPS3 protein from Arabidopsis revealed markedly increased activity in the presence of GTP. The addition of 1 mM GTP to the reaction mix resulted in maximal enzyme activation with CTP formation increasing nearly fivefold compared with assays carried out in the presence of only 0.05 mM GTP (Figure 6d). The maximal activity was determined to be 5.9 μmol CTP formed mg^{-1} protein h^{-1}.

When *CTPS3* was expressed as YFP fusion in *N. benthamiana* cells, filament formation was observed, whereas no corresponding filaments appeared in yeast cells (Figure 4). Therefore, we were curious to test whether recombinant, purified CTPS3 protein was able to form filaments. For this, the protein was incubated in the presence or absence of 5 mM CTP in the assay buffer. After the incubation, the sample was subjected to sequential ultracentrifugation at 50 000 and 100 000 ***g***. Supernatant and pellet fractions were collected and individually investigated by Western blotting and subsequent immunodetection using the aforementioned CTPS antibody to probe CTPS3 presence in either fraction. Interestingly, only after preincubation of the enzymatic reaction with its product CTP, CTPS3 could be detected in the 50 000 ***g*** pellet fraction (Figure 7). This indicates that CTP above a threshold level

promotes protein filament formation, which then, due to increased molecular weight, can precipitate in the pellet fraction. At 100 000 ***g*** no further CTPS3 protein accumulation was observed, proving that 50 000 ***g*** was sufficient to precipitate all protein filaments.

Arabidopsis isoform CTPS2 function is vital in particular developmental stages

Two independent homozygous T-DNA insertion mutants were successfully identified for loci *CTPS1*, *3* and *4*. In the case of *CTPS5* only a single T-DNA insertion line was isolated thus far. All lines were checked by polymerase chain reaction (PCR) for the presence of the T-DNA in both alleles of the corresponding gene (Figures S5 and S6). Furthermore, the absence of respective gene transcripts was verified by reverse transcription (RT)-PCR (Figure S7). Thus far, no phenotypic alterations in any of the aforementioned single-knockout mutants have been observed under short-or long-day growth conditions.

Interestingly, two T-DNA insertion lines from the GABI collection in *CTPS2* (GK032C02, GK156G07; Kleinboelting *et al.*, 2012) did not produce homozygous progeny. A corresponding segregation analysis (Table S1) led us to suppose that homozygous seeds of line GK032C02 do not germinate. As verified by PCR, a secondary reported insertion in the GABI line GK032C02 was successfully crossed out using a parental individual before carrying out respective segregation analysis. Therefore, it can be speculated that loss of *CTPS2* and not the secondary insertion cause seedling lethality in homozygote *ctps2–1* individuals. For *ctps2–2* the presence of only one T-DNA insertion was reported by GABI Kat (Kleinboelting *et al.*, 2012).

DISCUSSION

Arabidopsis harbors five putative CTPS isoforms (CTPS1–5), which are highly homologous among each other and to other CTPSs from prokaryotes and eukaryotic organisms across kingdoms (Liu, 2016). This finding is in line with previous reports on the conservation of proteins involved in purine or pyrimidine nucleotide synthesis (Moffatt and Ashihara, 2002). By heterologous expression of CTPS3 followed by an enzyme activity assay employing the purified CTPS3, we were able to confirm its CTPS activity. Taking into account the high sequence similarity among the Arabidopsis isoforms CTPS1–5 and the strict conservation of specific amino acid residues within the ALase and GATase domains known to be involved in substrate binding (Endrizzi *et al.*, 2005), it can be expected that all five Arabidopsis CTPS proteins exhibit CTPS activity.

Arabidopsis CTPS3 catalyzed a maximal activity of 5.9 μmol CTP mg^{-1} protein h^{-1}, which is far below the specific activity from *E. coli* CTPS (348 μmol CTP mg^{-1} protein h^{-1}; Barry *et al.*, 2014) or *S. cerevisiae* CTPS, respectively (39.6 μmol CTP mg^{-1} protein h^{-1}; Noree *et al.*, 2010). This points to a reduction in specific activity with increasing complexity of the organism. The substrate concentrations required to reach half-maximal activity are more alike those found for *E. coli* (Long and Pardee, 1967). The apparent affinity for ATP with 0.3 mM allows for high activity as the cytosolic concentration of ATP in the plant cytosol is in the range of 0.5–1 mM (Haferkamp *et al.*, 2006; Gout *et al.*, 2014). As ATP, the universal energy carrier, is usually kept at constant levels, it is rather unlikely that ATP exerts much control over CTPS activity. Gln, the other CTPS co-substrate, can be assumed to be non-

limiting as well. In contrast, UTP is an allosteric substrate ($K_{0.5}$ = 0.44 mM) and might well exert control over the enzyme reaction. Cytosolic UTP concentrations have been reported in the range of 0.05–0.5 mM in mammals (Pannbacker, 1967; Traut, 1994). In general, allosteric regulation allows for substrate-dependent fine-tuning. Similarly, the activator GTP is ideally suited to act as a control metabolite because half-maximal activation of CTPS3 activity occurs at physiological concentrations of the metabolite (Traut, 1994). Via this mechanism, the pyrimidine nucleotide UTP and the purine nucleotide GTP may exert a highly efficient CTPS control effect according to the demands of RNA biosynthesis, and in parallel ensure well-balanced cytosolic and thus cellular nucleotide pools.

Recently, much attention was drawn to the discovery of cytoophidia, filamentous protein structures formed by CTP synthesising enzymes from different organisms (Ingerson-Mahar *et al.*, 2010; Liu, 2010; Noree *et al.*, 2010; Azzam and Liu, 2013; Carcamo *et al.*, 2011; Barry *et al.*, 2014; Lynch *et al.*, 2017). One function of such structural organization is supposed to be a formerly not recognized additional level of enzyme activity regulation besides expression, phosphorylation (Park *et al.*, 1999; Kassel *et al.*, 2010) and metabolic regulation. In transient expression studies using CLSM with N- and C-terminal YFP fusions we gained visual evidence for the existence of protein filaments for CTPSs 3, 4 and 5 in plant cells. Intriguingly, the filament structures appeared to vary between isoforms and their formation was influenced by the location of the YFP tag. However, strikingly a similar behavior was never observed for CTPS1 or 2. Both isoforms remained fully soluble in the cytosol independent of YFP tag orientation or expression levels. This led us to conclude that the YFP tag itself is not responsible for filament formation.

Furthermore, we have shown that CTPS3-YFP fusion proteins remain active when synthesized in yeast (Figure S4). Therefore, it is unlikely that the YFP tag leads to misfolding of the protein. Based on our experimental outcomes, we therefore posit that filament formation is an exclusive feature of native Arabidopsis CTPS isoforms CTPS3, CTPS4 and CTPS5, which supposedly also occurs under *in vivo* conditions. It was shown for Drosophila that the N-terminal amino acid positions 2, 3 and 20 play an instructive role in filament formation (Huang *et al.*, 2017). A similar role for Arabidopsis CTPS1–5 can be doubted, as all of the corresponding amino acid positions in the highly conserved N-terminus are occupied by the identical residues found in Drosophila. However, CTPS1 and 2 clearly do not form filaments and thus indicated amino acids are unlikely to trigger filament formation.

In line with strict cytosolic localization of CTPSs from other eukaryotic organisms (Thomas *et al.*, 1988), we did not observe CTPS-YFP fusion proteins in any subcellular compartment. CTPSs can occur in a variety of high-molecular-weight structures, such as rods, rod and ring structures, filaments or as the so-called cytoophidia (Ingerson-Mahar *et al.*, 2010; Liu, 2010; Noree *et al.*, 2010; Azzam and Liu, 2013; Carcamo *et al.*, 2011; Barry *et al.*, 2014). In contrast, we mostly observed more unstructured, frazzled filaments or a cloudy appearance. It is possible that the YFP tag to some extent interferes with the polymerization preventing more uniform structures as observed in Drosophila or yeast cells. Intriguingly, the inability of CTPS3 and 4 to polymerize to filaments when expressed in yeast might indicate the existence of unknown organism-specific factors that influence the filamentation process.

Our results raise the question, why apparently two CTPS isoforms (CTPS1 and CTPS2) refrain to form filaments under the same experimental conditions that triggered filament formation in the three isoforms CTPS3–5. This feature may be explainable by minor variation in amino acid sequences of all isoforms. However, to answer this question more studies on purified protein from all five homologs are necessary. Detailed comparison to *E. coli* CTPS seems appropriate because this protein has been studied in detail with the help of cryo-EM structures of filaments. According to these analyses, one important element in filament formation is an alpha helix located between ALase and GATase domains named linker interface (Barry *et al.*, 2014). On the background of a generally high sequence similarity, this region is surprisingly low conserved in CTPSs of different origin, and this also holds true for the five Arabidopsis isoforms (Figure 1). Mutation of E227R in the *E. coli* enzyme reduced the ability for polymerization, and when this mutant replaced the native enzyme *E. coli* growth was disturbed. This phenomenon was explained by a lack of feedback inhibition of the mutated enzyme (Barry *et al.*, 2014). Applying homology modeling we identified amino acid residues in CTPS3 in the same linker-linker helix region where pyrG E227 locates. After mutation of those residues pointing to the protein periphery from this helix no altered filament formation behavior was observed (Figure S3). Obviously altering or omitting charges at single residues is not sufficient to disturb the polymerization mechanism in CTPS3, or this helix is not directly involved in polymerization of CTPS3 to filaments.

Unfortunately, we were not able to obtain indications of CTPS filament formation by *in situ* immunostaining experiments. This failure could be due to generally too low gene expression. Alternatively, CTPS filaments may form only in response to specific stress factors or they occur only spatially in distinct tissue or cell types. For instance, in Drosophila cytoophidia mostly occur in germline tissues (Azzam and Liu, 2013). Furthermore, special growth conditions might be required to induce filament formation. In *S. cerevisiae* it was shown that nitrogen starvation induces filament formation (Noree *et al.*, 2010). Expression studies in Arabidopsis reveal a marked upregulation of CTPS4 under drought stress (60-fold) and CTPS1 under salt stress (Zimmermann *et al.*, 2004). Besides abiotic stress, germination and embryo development are conditions in which cell division rates are high, and thus nucleotide synthesis must meet high CTP demands during DNA replication. Under such conditions CTPS1, 3 and 5 are upregulated (Zimmer-mann *et al.*, 2004; Johnston *et al.*, 2007).

The observed germination phenotype of the *CTPS2* T-DNA insertion line may indicate a special function of CTPS2 during germination that needs further detailed investigation in the future. Herein, it will be also important to try to pinpoint the exact stage in which plant development becomes affected. This will include to study to which degree CTPS activity might be crucial for full fertility. An important role for CTPS2 during seed germination is supported by a fourfold upregulation during a 48 h stratification treatment (Zimmermann *et al.*, 2004). In this study, no additional phenotypes of other CTPS isoforms could be detected. However, so far mutants were investigated strictly under short- or long-day condition without application of any kind of stress. It is conceivable that specific, yet to be determined, stress triggers may result in observable phenotypes even in single mutants. Another likely explanation is that loss-of-function in single CTPS genes can be overcome to some extent by

functional redundancy among the five gene family members. Genetic functional redundancy is well described in plant gene families, but could be tested by designing higher-order *ctps* mutants at a given time (Cutler and McCourt, 2005).

In summary, here we presented the initial characterization of the five loci encoding for CTPS enzymes in the model plant *A. thaliana*. Our results show that plants, different from other organisms, seem to have very distinct CTPS protein members that either are capable to form filamentous structures or remain soluble under every condition tested. Furthermore, all plant CTPS members failed to form characteristic cytoophidia filaments in yeast. This opens up the possibility that secondary protein or co-substrate binding are required for filament formation of the plant enzymes in yeast cells. Because an upregulation of CTPS activity was recognized in cancer cells and resistance to some cytotoxic drugs is based on specific CTPS mutations, deciphering the exact regulation of CTPS activity and the role of filament formation remains an important scientific issue (Williams *et al.*, 1978). Based on our data, we encourage the expansion of research of CTPS filament formation towards including plant CTPS members. Due to their strict separation in filament-forming and soluble protein categories they may allow for critical insights into the role and function of filament-forming CTPS enzymes in the future.

EXPERIMENTAL PROCEDURES

Plant growth

For DNA isolation, tissue collection and phenotypic inspection, wild-type and transgenic *A. thaliana* (L.) Heynh. plants (ecotype Columbia) were grown in standardized ED73 (Einheitserde und Humuswerke Patzer, Buchenberg, Germany) soil under short-day conditions (120 µmol quanta m^{-2} sec^{-1} in a 10 h light/14 h dark regime, temperature 22°C, humidity 60%). Prior to germination, seeds were incubated for 24 h in the dark at 4°C for imbibition (Weigel and Glazebrook, 2002). *Nicotiana benthamiana* plants were grown under the same conditions.

T-DNA insertion lines

T-DNA insertion lines from the Salk, SAIL and GABI-KAT collection were used (Sessions *et al.*, 2002; Alonso *et al.*, 2003; Kleinboelting *et al.*, 2012). The following lines were studied: *ctps1–1* = SALK_031868; *ctps1–2* = SAIL_623_E09; *ctps2–1* = GK032C02; *ctps3–1* = SALK_118507; *ctps3–2* = GK_534A02; *ctps4–1* = SALK_020074C; *ctps4–2* = SALK_127028C; *ctps5–1* = SAIL_645_D02. Primers used for PCR testing for the presence of the T-DNA insertion and the homozygous state are listed in Table S2.

Cloning of CTPSs

Cloning of the five full-length CTPSs from *A. thaliana* was carried out using cDNA pools as template or genomic DNA in the case of extremely low expressed *CTPS5*, respectively. Sequences of gene-specific primers with restriction sites are provided in Table S2. Initially, cDNA products were subcloned into pJET1.2 (Thermo Fisher, Waltham, MA, USA). In the case of *CTPS1* a silent mutation was added to destroy an internal XmaI site that prevented cloning of the N-terminal fusion. Subsequently *CTPS* genes were cloned into either N- or C-

terminal frame with Venus (YFP) via indicated restriction sites. The binary plasmid used for *in planta* expression were pBARII_UT_mVenusN vector in the case of N-terminal translational YFP fusions (Waadt *et al.*, 2015) or for C-terminal translational YFP fusions pHygII_UT_mVenusC (Kunz *et al.*, 2014). YFP fusion constructs were then transformed into *Agrobacterium tumefaciens* strain GV3101.

For CTPS1–4 and Ura7/Ura8 expression studies in yeast, corresponding full-length cDNAs were cloned into pYe_T_VenusC (kind gift of Dr Rainer Waadt) using the primers listed in Table S2. Constructs were then transformed into *S. cerevisiae* W303, and resulting colonies were picked from selection plates and transferred to full nutrition medium (YPD). Yeast cells were monitored by CLSM.

A CTPS3 construct for heterologous expression in *E. coli* strain BLR(DE3)-pLysS (Studier and Moffatt, 1986) was generated by amplifying full-length CTPS3 with CTPS3-pET containing 5'XhoI and 3'XhoI restriction sites. After XhoI digest the resulting fragment was introduced into pET16b (Novagen, Heidelberg) opened with the same enzyme. The resulting construct contains an N-terminal 10×-His-Tag.

Transient expression in *Nicotiana benthamiana*

Transient expression of *CTPS* genes fused to YFP was performed as detailed in Witte *et al.* (2004). *Agrobacterium tumefaciens* strain GV3101 prior transformed with CTPS N- or C-terminal YFP constructs was infiltrated through the lower epidermis of 6-week-old *N. benthamiana* leaves. After 3 days leaves were analyzed for the presence of fluorescence signals with a Leica TCS SP5II microscope (514 nm excitation and 525–582 nm detection of emission through a HCX PL APO 63 × 1.2 W water immersion objective). Chlorophyll autofluorescence was detected with 514 nm excitation and a 651–704 nm emission wavelength. Subsequently, correct protein sizes were verified in total protein extracts by immunodetection using an α-eGFP primary antibody and a HRP-coupled secondary antibody (anti-rabbit; see also 'Western blotting' section for additional information).

In the case of yeast, cells were inspected through a HCX PL APO 63 × 1.4−0.6 OIL immersion objective with the same settings as described above.

CTPS3 expression in *Escherichia coli* and protein purification

Escherichia coli BLR cells transformed with a HIS_{10}-CTPS3 pET16b construct were grown overnight at 37°C in YT medium and used to inoculate 1 L TB medium to an OD600 of 0.08. Cells were grown to an OD of 2, transferred to 18°C and incubated under constant shaking for another hour. Gene expression was induced by 0.5 mM IPTG and cultivation proceeded for another 18–20 h. Then cells were harvested and resuspended in 1.5-fold the pellet volume with lysis buffer (1 M NaCl, 50 mM Hepes, pH 7.6; 20 mM imidazole, 10% glycerol; 0.2 mM PMSF and Dnase). Cells were broken by sonication and debris pelleted at 35.00 g for 30 min under cooling. The supernatant was incubated with Ni-sepharose 6 fast flow (GE Healthcare, Freiburg, Germany) equilibrated according to the manufacturer's protocol. After washing, CTPS3 was eluted with a stepped gradient of imidazole (70–600 mM). The fractions containing 210–250 mM imidazole were combined, desalted in activity buffer and stored at 4°C for further use.

Biochemical assay

Purified CTPS3 (50 µl at 0.5 mg protein ml^{-1}) or yeast extracts of *CTPS3*-expressing cells were preincubated for 10 min in activity buffer [Hepes-KOH pH 7.6 (50 mM), $MgCl_2$ (5 mM), KCl (150 mM), UTP (2 mM), GTP (0.2 mM), dithiothreitol (DTT) (2 mM)]. Subsequently, ATP (2 mM) and glutamine (20 mM) were added to start the reaction. At indicated time points the reaction was stopped by heating the sample for 5 min (95°C). Samples were centrifuged (20 000 ***g***, 10 min) and stored at −80°C for measurement. Separation and quantification of reaction products was achieved by HPLC runs on a Dionex system equipped with a Nucleodur 100-(5C18ec 250/4) column and isocratic elution with 10% NaAc (100 mM, pH5.8), 90% acetonitrile and UV detection at 265 nm.

Western blotting

Twenty microgram total protein was separated on sodium dodecyl sulfate (SDS)–polyacrylamide gel electrophoresis (PAGE) and blotted onto nitrocellulose membrane by wet blotting. Blocking was achieved by incubation in 3% milk powder (w/v) in TBS (Tris-HCl, pH 7.5; NaCl, 150 mM; 0.1% Tween 20 in TBST). Washings were performed in TBS, TBST, TBS 10 min each. As primary antibody, eGFP monoclonal antibody (MAB 3580, Merck, Darmstadt, Germany), CTPS-specific polyclonal (Santa Cruz sc-134457) or anti-HIS (SAB 1306085, Sigma-Aldrich) ab were used. As secondary ab, anti-rabbit-HRP was used and detection of chemiluminescence was performed in a Fusion Solo S6 (Vilber-Lourmat, VWR) imager.

Centrifugation assay

Recombinant, purified CTPS3 protein (0.5 mg ml^{-1}) was incubated in the presence or absence of CTP (5 mM) in activity buffer [Hepes-KOH pH 7.6 (50 mM), $MgCl_2$ (5 mM), KCl (150 mM), UTP (2 mM), GTP (0.2 mM), DTT (2 mM)]. After the incubation, the sample was subject to sequential centrifugation at 50 000 and 100 000 ***g***. CTPS3 protein in supernatants and pellet fractions was separated from other proteins via SDS gel electrophoresis, and subsequently detected using immunodetection with anti His-Tag antibody followed by color detection (NBT, BCIP).

Supplementary Material

Refer to Web version on PubMed Central for supplementary material.

ACKNOWLEDGEMENTS

The work was supported by DFG-grant MO 1032/4–1 and IRTG 1830 to T.M., and an NSF Career Award IOS-1553506 to H.-H.K.H.-H.K. is grateful for early project advice by Dr Jim Wilhelm UCSD. R.A.D. received funding from the NIH Biotechnology Training Program at WSU and from the NSF Graduate Research Fellowship Program. The authors thank Dr Rainer Waadt for kindly providing pYE_T_Venus. The authors thank Leo Bellin and Moritz Krämer for supporting mutant screening and segregation analysis. The authors gratefully acknowledge generous support of the work by Prof. H. Ekkehard Neuhaus.

REFERENCES

Alonso JM, Stepanova AN, Leisse TJ, Kim CJ and Chen H (2003) Genome-wide insertional mutagenesis of Arabidopsis thaliana. Science 301, 653–657. [PubMed: 12893945]

Aughey GN, Grice SJ, Chen QS et al. (2014) Nucleotide synthesis is regulated by cytoophidium formation during neurodevelopment and adaptive metabolism. Biol. Open 3, 1045–1056. 10.1242/bio.201410165. [PubMed: 25326513]

Azzam G and Liu JL (2013) Only one isoform of *Drosophila melanogaster* CTP synthase forms the cytoophidium. PLoS Genet 9, e1003256 10.1371/journal.pgen.1003256. [PubMed: 23459760]

Barry RM, Bitbol AF, Lorestani A et al. (2014) Large-scale filament formation inhibits the activity of CTP synthetase. Elife 3, e03638 10.7554/eLife.03638. [PubMed: 25030911]

Carcamo WC, Satoh M, Kasahara H et al. (2011) Induction of cytoplasmic rods and rings structures by inhibition of the CTP and GTP synthetic pathway in mammalian cells. PLoS ONE 6, e29690 10.1371/journal.pone.0029690. [PubMed: 22220215]

Cutler S and McCourt P (2005) Dude, where's my phenotype? Dealing with redundancy in signaling networks. Plant Physiol 138, 558–559. 10.1104/pp.104.900152. [PubMed: 15955914]

Endrizzi JA, Kim H, Anderson PM and Baldwin EP (2004) Crystal structure of *Escherichia coli* cytidine triphosphate synthetase, a nucleotide-regulated glutamine amidotransferase/ATP-dependent amidoligase fusion protein and homologue of anticancer and antiparasitic drug targets. Biochemistry 43, 6447–6463. [PubMed: 15157079]

Endrizzi JA, Kim H, Anderson PM and Baldwin EP (2005) Mechanisms of product feedback regulation and drug resistance in cytidine triphosphate synthetases from the structure of a CTP-inhibited complex. Biochemistry 44, 13 491–13 499.

Evans DR and Guy HI (2004) Mammalian pyrimidine biosynthesis: fresh insights into an ancient pathway. J. Biol. Chem 279, 33 035–33 038.

Gout E, Rebeille F, Douce R and Bligny R (2014) Interplay of Mg2+, ADP, and ATP in the cytosol and mitochondria: unravelling the role of Mg2+ in cell respiration. Proc. Natl Acad. Sci. USA 111, E4560–E4567. [PubMed: 25313036]

Haferkamp I, Schmitz-Esser S, Wagner M, Neigel N, Horn M and Neuhaus HE (2006) Tapping the nucleotide pool of the host: novel nucleotide carrier proteins of *Protochlamydia amoebophila*. Mol. Microbiol 60, 1534–1545. [PubMed: 16796686]

Huang Y, Wang JJ, Ghosh S and Liu JL (2017) Critical roles of CTP synthase N-terminal in cytoophidium assembly. Exp. Cell Res 354, 122–133. [PubMed: 28342900]

Ingerson-Mahar M, Briegel A, Werner JN, Jensen GJ and Gitai Z (2010) The metabolic enzyme CTP synthase forms cytoskeletal filaments. Nat. Cell Biol 12, 739–746. [PubMed: 20639870]

Johnston AJ, Meier P, Gheyselinck J et al. (2007) Genetic subtraction profiling identifies genes essential for Arabidopsis reproduction and reveals interaction between the female gametophyte and the maternal sporophyte. Genome Biol 8, R204. [PubMed: 17915010]

Kassel KM, Au DR, Higgins MJ, Hines M and Graves LM (2010) Regulation of human cytidine triphosphate synthetase 2 by phosphorylation. J. Biol. Chem 285, 33 727–33 736.

Kleinboelting N, Huep G, Kloetgen A, Viehoever P and Weisshaar B (2012) GABI-Kat SimpleSearch: new features of the *Arabidopsis thaliana* T-DNA mutant database. Nucleic Acids Res 40(Database issue), D1211–D1215. 10.1093/nar/gkr1047. [PubMed: 22080561]

Kunz H-H, Zamani-Nour S, Häusler RE et al. (2014) Loss of cytosolic phosphoglucose isomerase affects carbohydrate metabolism in leaves and is essential for fertility of Arabidopsis. Plant Physiol 166, 753–765. 10.1104/pp.114.241091. [PubMed: 25104722]

Levitzki A and Koshland DE Jr (1972) Ligand-induced dimer-to-tetramer transformation in cytosine triphosphate synthetase. Biochemistry 11, 247–253. [PubMed: 4550560]

Liebermann I (1956) Enzymatic amination of uridine triphosphate to cytidine triphosphate. J. Biol. Chem 222, 765–775. [PubMed: 13367044]

Liu JL (2010) Intracellular compartmentation of CTP synthase in Drosophila. J. Genet. Genomics 37, 281–296. [PubMed: 20513629]

Liu JL (2011) The enigmatic cytoophidium: compartmentation of CTP synthase via filament formation. BioEssays 33, 159–164. [PubMed: 21254152]

Liu JL (2016) The cytoophidium and its kind: filamentation and compartmentation of metabolic enzymes. Ann. Rev. Cell Dev. Biol 32, 349–372. [PubMed: 27362644]

Long CW and Pardee AB (1967) Cytidine triphosphate synthetase of *Escherichia coli* B. I. Purification and kinetics. J. Biol. Chem 242, 4715–4721. [PubMed: 4862983]

Lunn FA, MacDonnell JE and Bearne SL (2008) Structural requirements for the activation of *Escherichia coli* CTP synthase by the allosteric effector GTP are stringent, but requirements for inhibition are lax. J. Biol. Chem 283, 2010–2020. [PubMed: 18003612]

Lynch EM, Hicks DR, Shepherd Met al. (2017) Human CTP synthase filament structure reveals the active enzyme conformation. Nat. Struct. Mol. Biol 24, 507–514. [PubMed: 28459447]

Moffatt BA and Ashihara H (2002) Purine and pyrimidine nucleotide synthesis and metabolism. The Arabidopsis Book 1: e0018. [PubMed: 22303196]

Noree C, Sato BK, Broyer RM and Wilhelm JE (2010) Identification of novel filament-forming proteins in *Saccharomyces cerevisiae* and *Drosophila melanogaster*. J. Cell Biol 190, 541–551. [PubMed: 20713603]

Noree C, Monfort E, Shiau AK and Wilhelm JE (2014) Common regulatory control of CTP synthase enzyme activity and filament formation. Mol. Biol. Cell 25, 2282–2290. 10.1091/mbc.E14-04-0912. [PubMed: 24920825]

Pannbacker RG (1967) Uridine diphosphoglucose biosynthesis during differentiation in the cellular slime mold. II. In vitro measurements. Biochemistry 6, 1287–1293. [PubMed: 6068283]

Park TS, Ostrander DB, Pappas A and Carman GM (1999) Identification of Ser424 as the protein kinase A phosphorylation site in CTP synthetase from Saccharomyces cerevisiae. Biochemistry 38, 8839–8848. [PubMed: 10393561]

Schmid M, Davison TS, Henz SRet al. (2005) A gene expression map of *Arabidopsis thaliana* development. Nat. Genet 37, 501–506. [PubMed: 15806101]

Sessions A, Burke E, Presting Get al. (2002) A high-throughput arabidopsis reverse genetics system. Plant Cell 14, 2985–2994. 10.1105/tpc.004630. [PubMed: 12468722]

Studier FW and Moffatt BA (1986) Use of bacteriophage T7 RNA polymerase to direct selective high-level expression of cloned genes. J. Mol. Biol 189, 113–130. [PubMed: 3537305]

Thomas PE, Lamb BJ and Chu EH (1988) Purification of cytidine-triphosphate synthetase from rat liver, and demonstration of monomer, dimer and tetramer. Biochim. Biophys. Acta 953, 334–344. [PubMed: 3355843]

Thompson JD, Higgins DG and Gibson DJ (1994) CLUSTAL W: improving the sensitivity of progressive multiple sequence alignment through sequence weighting, position specific gap penalties and weight matrix choice. Nucleic Acids Res 22, 4673–4680. [PubMed: 7984417]

Traut TW (1994) Physiological concentrations of purines and pyrimidines. Mol. Cell. Biochem 140, 1–22. [PubMed: 7877593]

Waadt R, Manalansan B, Rauniyar Net al. (2015) Identification of open stomata1-interacting proteins reveals interactions with sucrose non-fermenting1-related protein Kinases2 and with Type 2A protein phosphatases that function in abscisic acid responses. Plant Physiol 169, 760–779. 10.1104/pp.15.00575. [PubMed: 26175513]

Wadskov-Hansen SL, Willemoes M, Martinussen J, Hammer K, Neuhard J and Larsen S (2001) Cloning and verification of the *Lactococcus lactis pyrG* gene and characterization of the gene product, CTP synthase. J. Biol. Chem 276, 38 002–38 009.

Weigel D and Glazebrook J (2002) Arabidopsis. A Laboratory Manual New York: Cold Spring Harbor Laboratory Press.

Williams JC, Kizaki H, Weber G and Morris HP (1978) Increased CTP synthetase activity in cancer cells. Nature 271, 71–73. [PubMed: 203856]

Witte CP, Noel LD, Gielbert J, Parker JE and Romeis T (2004) Rapid one-step protein purification from plant material using the eight-amino acid StrepII epitope. Plant Mol. Biol 55, 135–147. [PubMed: 15604670]

Zimmermann P, Hirsch-Hoffmann M, Henning L and Gruissem W (2004) Genevestigator. Arabidopsis microarray database and analysis toolbox. Plant Physiol 136, 2621–2632. [PubMed: 15375207]

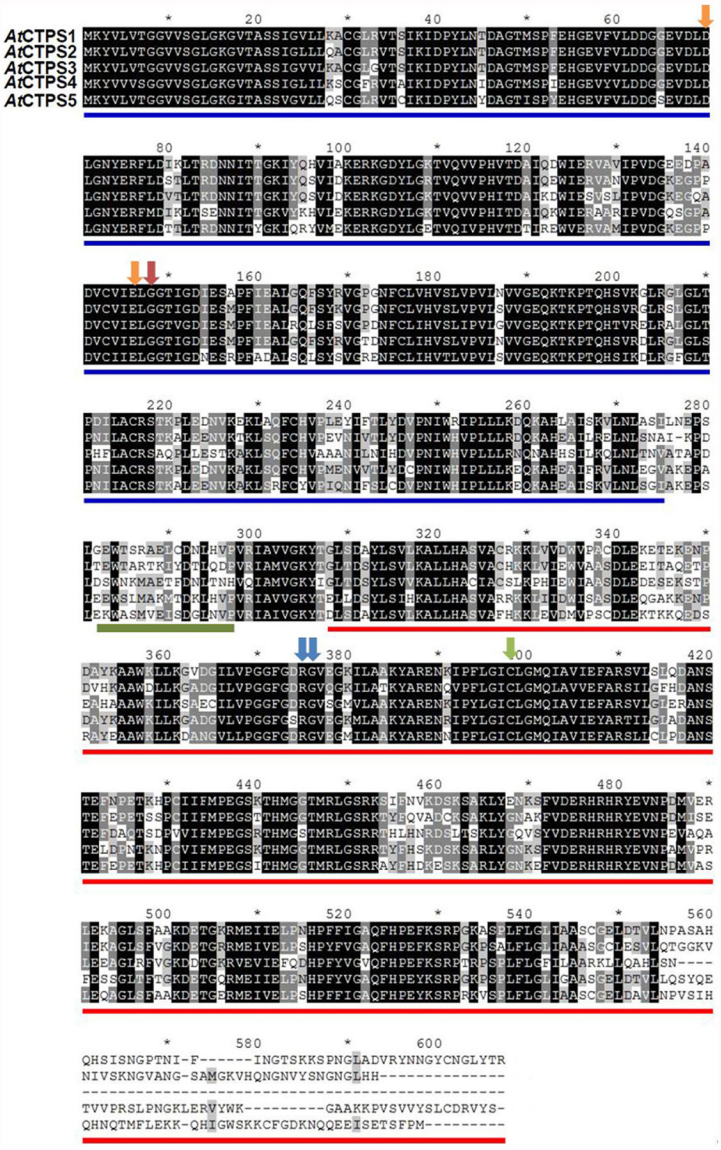

Figure 1.

Alignment of the five Arabidopsis cytidine triphosphate synthases (CTPSs). Arabidopsis CTPSs 1–5 were aligned by ClustalW (Thompson *et al.*, 1994). Identical amino acid positions in all sequences are shown with black background, similar amino acids in gray background. Visualization was achieved by Gene Doc. Ammonia ligase domain is marked by blue line, glutamine amidotransferase domain by red line. Arrows show conserved positions for substrate and effector binding; ATP (orange), UTP (red), GTP (blue) and catalysis (green). The linker-linker interface is indicated by a green bar.

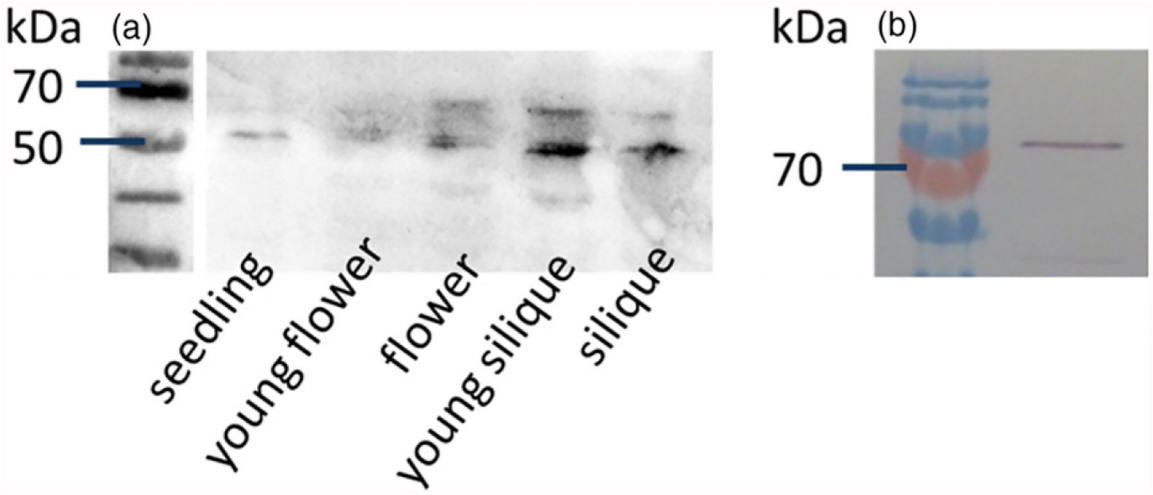

Figure 2.

Western blot of Arabidopsis tissue extracts probed with anti-cytidine triphosphate synthase (CTPS) antibody.

(a) Tissue was collected from Arabidopsis Col-0 plants grown under short-day conditions for 4 weeks and then transferred to long-day growth for flower induction; 20 μg of total protein extracts from indicated tissues was loaded per lane. Primary anti-CTPS antibody (1:100, sc-134457; Santa Cruz) was used followed by secondary HRP-antibody-dependent detection via chemiluminescence.

(b) Extract from CTPS3-YFP-expressing yeast cells, probed with the antibody used in (a). [Colour figure can be viewed at wileyonlinelibrary.com].

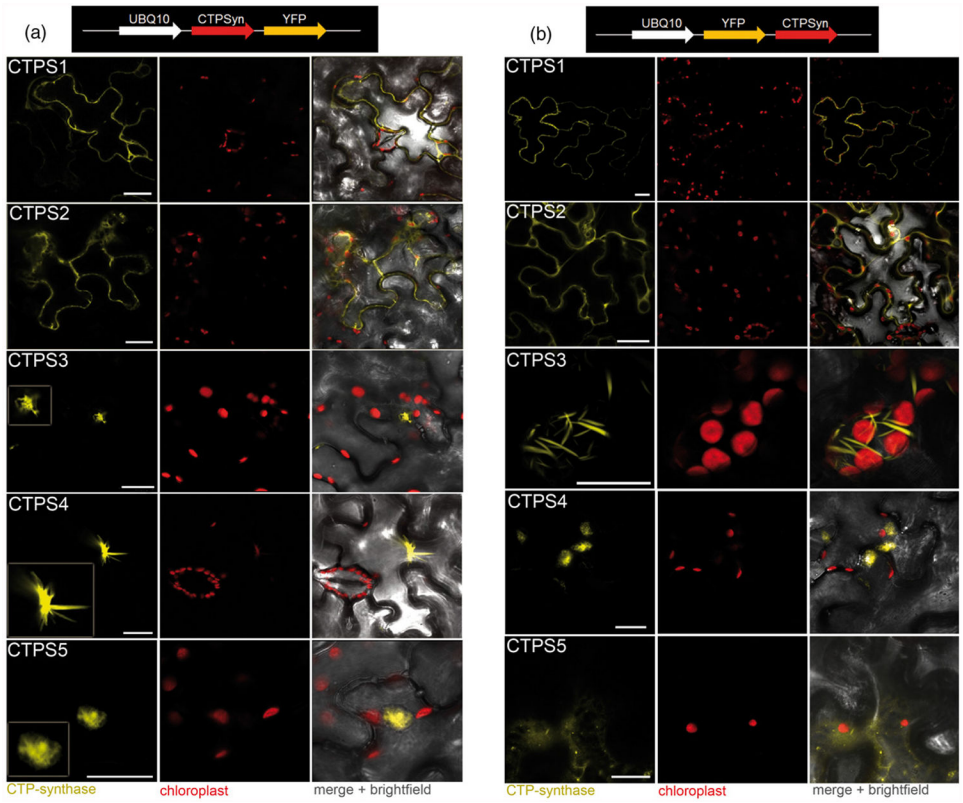

Figure 3.

Cytidine triphosphate synthase (CTPS) C-terminal (a) and N-terminal (b) fusion to YFP expressed in *Nicotiana benthamiana* leaves. Corresponding constructs were transformed into Agrobacterium strain GV31301 and subsequently co-infiltrated into leaves. After 3–4 days, epidermis cells of intact leaves were monitored by confocal laser-scanning microscopy (CLSM) as given in Experimental procedures. Scale bar: 20 μm.

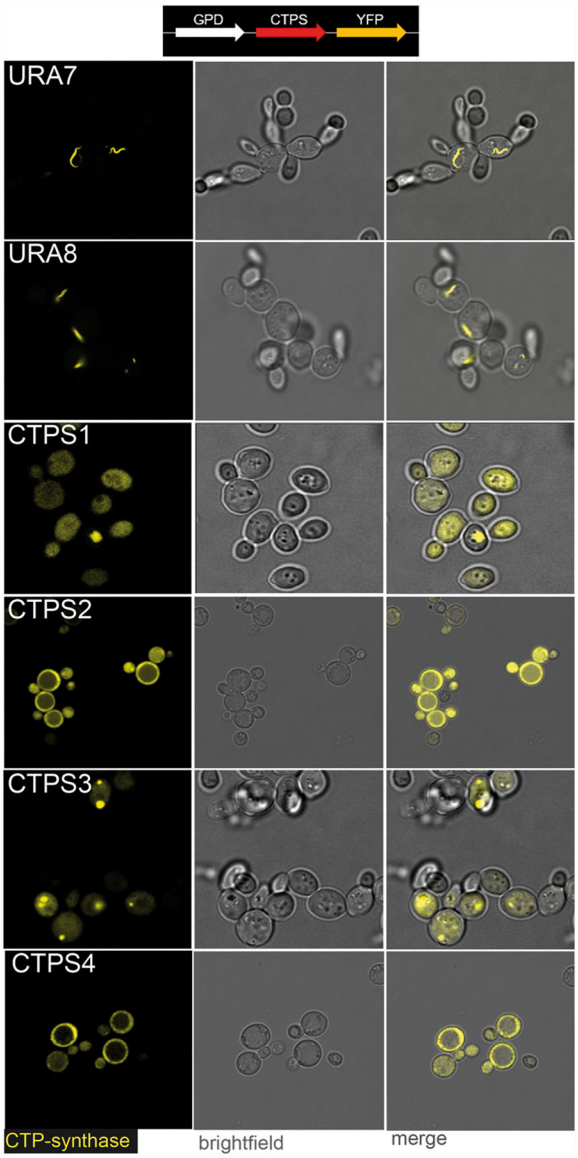

Figure 4.

Yeast Ura7, Ura8 and Arabidopsis cytidine triphosphate synthase (CTPS)1–4 C-terminal fusion to YFP expressed in *Saccharomyces cerevisiae*. Constructs were transformed into *S. cerevisiae* W303, and resulting colonies were picked from selection plates and transferred to full nutrition medium (YPD). Yeast cells were monitored by confocal laser-scanning microscopy (CLSM) as given in Experimental procedures. Yeast cells shown are 5–7 μm in diameter.

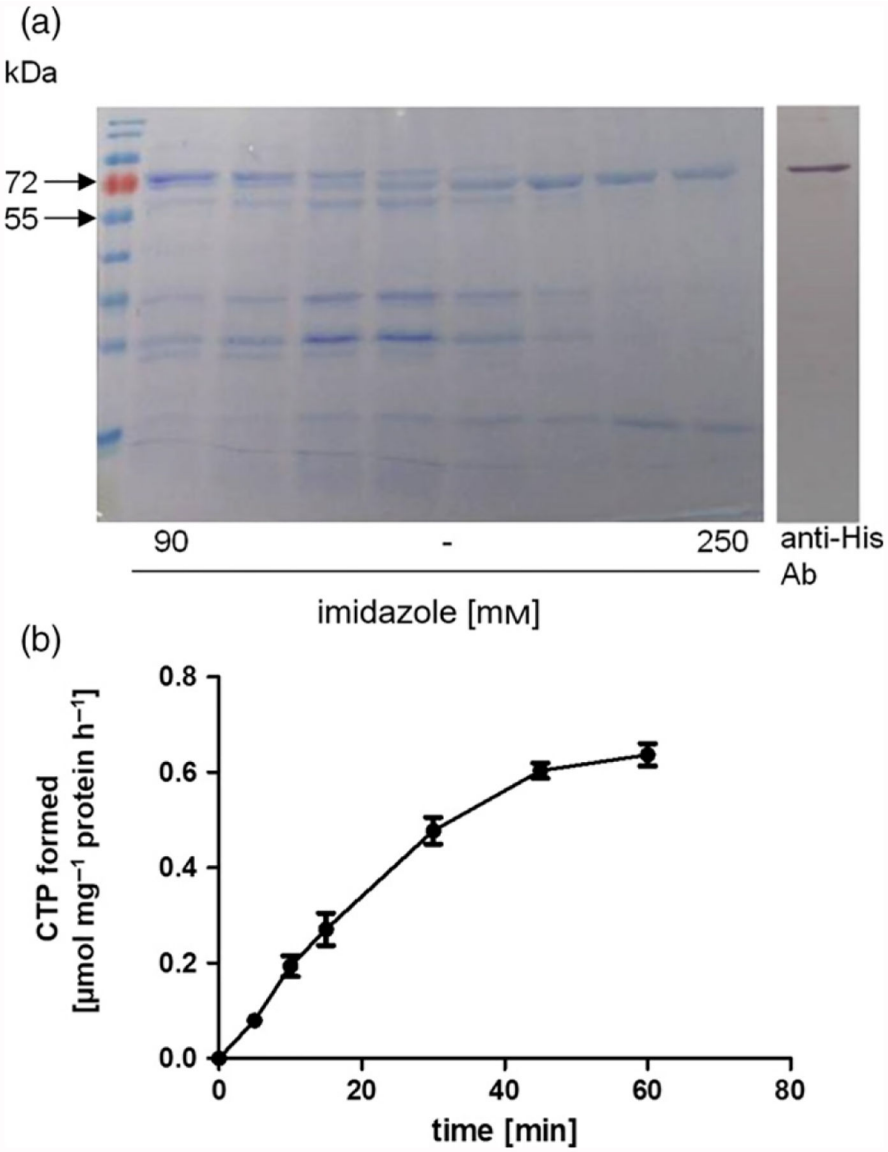

Figure 5.

Purification of recombinant cytidine triphosphate synthase (CTPS) 3 protein and determination of its catalytic activity.

(a) Elution of CTPS3 from Ni-Sepharose by stepwise increasing imidazole concentration visualized by Coomassie stain of sodium dodecyl sulfate (SDS)–polyacrylamide gel electrophoresis (PAGE). Western blot with anti-His antibody (right panel).

(b) CTPS activity was determined as given in Experimental procedures. Reaction products were separated and quantified by high-performance liquid chromatography (HPLC). The reaction contained UTP (4 mM), Gln (20 mM), ATP (2 mM) and GTP (0.2 mM). Results show the mean values of three independent experiments (± SE).

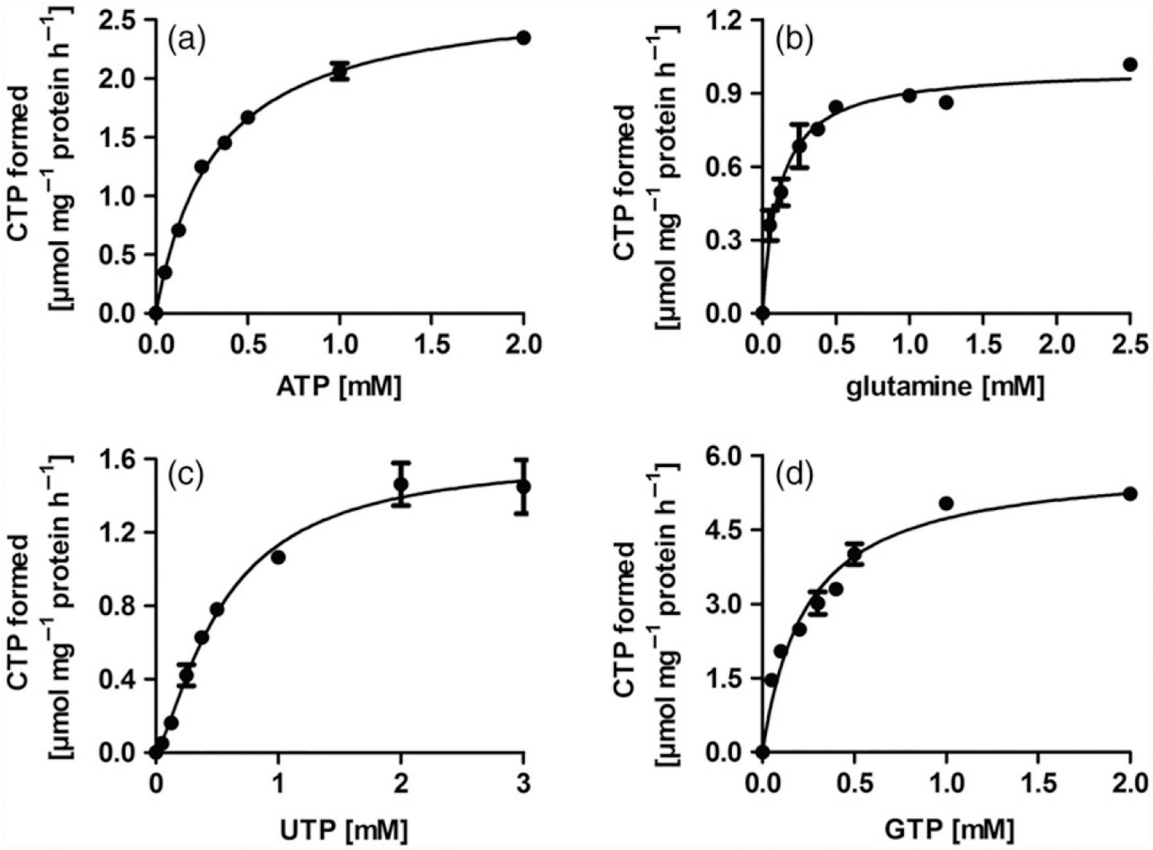

Figure 6.

Biochemical characterization of purified, recombinant cytidine triphosphate synthase (CTPS)3 protein.

CTPS3 protein (0.5 mg ml^{-1}) was incubated as given in Experimental procedures with UTP (4 mM), Gln (20 mM), ATP (2 mM) and GTP (0.2 mM) if not indicated otherwise. Values at the *y*-axis are given as µmol CTP generated mg^{-1} protein h^{-1}. The results represent mean values obtained in three independent experiments (± SE).

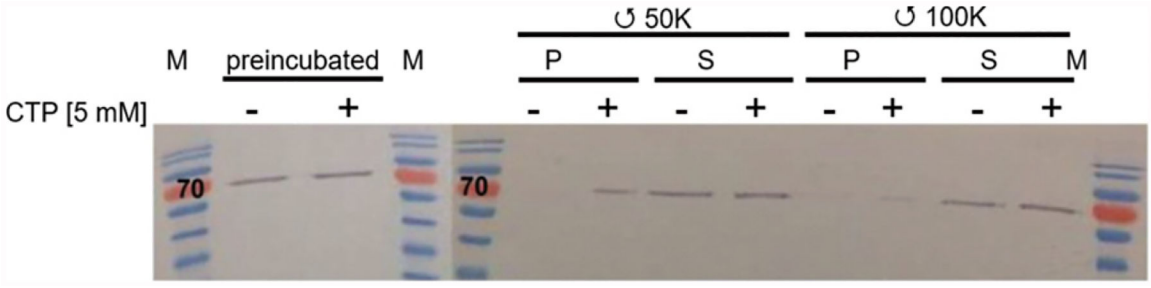

Figure 7.

Ultracentrifugation assay with purified recombinant cytidine triphosphate synthase (CTPS)3 protein.

CTPS3 (1 mg ml^{-1}) was incubated with or without the addition of CTP (5 mM) for 15 min. Samples were subjected to ultracentrifugation at the indicated *g*-force. Pellet (P) and supernatant (S) were separated on a gel, blotted and probed with anti-His antibody. CTPS3 was found in the pellet after ultracentrifugation at 50 000 ***g*** only if 5 mM CTP was added to the assay.

Table 1

Sequence identity between Arabidopsis and previously characterized CTPSs from other organisms

AGI, Protein	Ura7	Ura8	CTPS1	CTPS2	Isoform A	Isoform B	PyrG
A*t1g*30820, CTPS1	54.23	54.15	54.82	55.63	53.77	46.90	48.87
*At3g*12670, CTPS2	56.65	54.50	56.01	54.95	54.33	47.00	46.89
A*t4g*02120, CTPS3	54.33	51.36	53.47	52.22	52.26	45.06	47.93
*At4g*20320, CTPS4	54.92	55.36	57.02	55.97	53.98	46.70	47.93
*At2g*34890, CTPS5	56.83	55.56	58.45	55.76	55.04	47.30	46.62

Sequences were compared with ClustalW software. CTPSs from *Saccharomyces cerevisiae* [URA7 (P28274); URA8 (P38627)], *Homo sapiens* [CTPS1 (P17812); CTPS2 (Q9NRF8)], *Drosophila melanogaster* [Isoform A; B (CG6854)] and *Escherichia coli* [(PYRG (P0A7E5)] were used. Sequence identity is given in (%).

CTPS, cytidine triphosphate synthase.